Colloid Polym Sci (2007) 285:1683–1690
DOI 10.1007/s00396-007-1742-5

ORIGINAL CONTRIBUTION

Synthesis and characterization of side-chain cholesteric elastomers derived from an isosorbide crosslinking agent

Bao-Yan Zhang · Jian-She Hu · Bai Wang · Dan-Shu Yao · Hao Li

Received: 9 February 2007 / Revised: 26 May 2007 / Accepted: 9 July 2007 / Published online: 5 September 2007

Abstract New liquid crystalline monomer 4-(4-ethoxybenzoyloxy)biphenyl-4′-[(10-undecylen-1-yloxy)-4′-ethoxy] benzoate (**M$_1$**), chiral crosslinking agent isosorbide di-(10-undecylen-1-yloxybenzoate) (**M$_2$**), and the corresponding elastomers were prepared. The chemical structures of **M$_1$** and **M$_2$** were characterized by Fourier transform infrared and ^{1}H-nuclear magnetic resonance. The mesomorphic properties and phase behavior were investigated by differential scanning calorimetry, thermogravimetric analysis, polarizing optical microscopy, and X-ray diffraction measurements. **M$_1$** exhibited typical threaded texture and droplet texture of nematic phase. The use of chiral crosslinking agent in the polymer networks could induce cholesteric phase. The elastomers containing less than 10 mol% of the chiral crosslinking units showed elasticity, reversible phase transition, wide mesophase temperature ranges, and high thermal stability. For the elastomers **P$_2$**–**P$_4$**, the glass transition temperature (T_g) increased; clearing temperature (T_i) and mesophase temperature range (ΔT) decreased with increasing content of the crosslinking unit.

Keywords Liquid crystalline · Chiral · Crosslinking · Elastomers · Cholesteric phase

Introduction

Since the synthesis of liquid crystalline elastomers (LCEs) was reported by Finkelmann in 1981 [1], research into LCEs, mainly using polysiloxanes, polyacrylates, polymethacrylates, and polyurethane as polymer backbone, has expanded rapidly as a new class of LC materials because they give rise to macroscopic features [1–7]. In the past decade, chiral LCEs have attracted considerable interest because of their remarkable electromechanical properties and potential applications in numerous areas, especially in the fields of nonlinear optical devices, full-color thermal imaging, electrooptical materials, and fast switching [8–16]. Chiral LCEs combine basic features of polymer networks with the physical properties of chiral LC compounds. From a scientific point of view, chiral LCEs are fascinating because they allow a study of the interplay of electrical and mechanical forces in a rubbery material. This happens because the reorientation of the mesogenic groups in the electric field creates stress in the network of the polymer chains. As a branch of chiral LCEs, cholesteric LCEs show piezoelectricity [17–20], tunable mirrorless lasing [21, 22], and photonics [23, 24] besides conventional mechanical properties. Cholesteric LCEs have the potential to act as a device that transforms a mechanical signal into an electric signal and are considered as a candidate for new piezoelectric materials.

Isosorbide has been used as a chiral center for the synthesis of main-chain cholesteric LC polymers [25–30]. However, to the best of our knowledge, research on side-chain cholesteric LC polymers or elastomers derived from isosorbide derivates was little reported [31–33]. The aims of our research were: (1) to synthesize new cholesteric LCEs derived from an isosorbide crosslinking agent; (2) to study structure–property relationships of cholesteric LCEs; and (3) to explore applications as novel piezoelectric device in the future. In a previous study, we reported the synthesis and properties of side-chain cholesteric LCEs derived from a nematic, smectic, and nonmesogenic crosslinking agent,

B.-Y. Zhang (✉) · J.-S. Hu · B. Wang · D.-S. Yao · H. Li
Center for Molecular Science and Engineering,
Northeastern University,
Shenyang 110004, People's Republic of China
e-mail: byzcong@163.com

respectively [34–37]. In this study, a series of new side-chain cholesteric LCEs, derived from an isosorbide derivate as a chiral crosslinking agent, were synthesized. The LC properties of the monomers and elastomers obtained were characterized with differential scanning calorimetry (DSC), thermogravimetric analysis (TGA), polarizing optical microscopy (POM), and X-ray diffraction (XRD). The effect of the content of the chiral crosslinking unit on the phase behavior of the elastomers is discussed.

Experimental

Materials

Polymethylhydrosiloxane (PMHS, $\overline{M_n}$=700–800) was purchased from Jilin Chemical Industry. Undecylenic acid was purchased from Beijing Jinlong Chemical Reagent. 4,4′-Dihydroxybiphenyl (from Aldrich) was used as received. Isosorbide was purchased from Jiangxi Haohe Chemical Industry and was dried over P_4O_{10} in *vacuum* before use. Toluene used in the hydrosilylation reaction was purified by treatment with $LiAlH_4$ and distilled before use. All solvents and reagents were purified by standard methods.

Measurements

Fourier transform infrared spectra were measured on a Perkin-Elmer spectrum One (B) spectrometer (Perkin-Elmer, Foster City, CA). ^{1}H-nuclear magnetic resonance (NMR; 400 MHz) spectra were obtained with a Varian WH-90PFT spectrometer (Varian Associates, Palo Alto, CA). The elemental analysis was carried out with an Elementar Vario EL III (Elementar, Germany). The optical rotations were obtained on a Perkin-Elmer 341 polarimeter. The phase transition temperatures and thermodynamic parameters were determined with a Netzsch DSC 204 (Netzsch, Germany) equipped with a liquid nitrogen cooling system. The heating and cooling rates were 10 °C/min. The thermal stability of the polymers with nitrogen atmosphere was measured with a Netzsch TGA 209C thermogravimetric analyzer. The heating rates were 20 °C/min. A Leica DMRX (Leica, Germany) POM equipped with a Linkam THMSE-600 (Linkam, England) cool and hot stage was used to observe phase transition temperatures and analyze LC properties through observation of optical textures. XRD measurements were performed with a nickel-filtered Cu Kα (λ=1.542 Å) radiation with a DMAX-3A Rigaku (Rigaku, Japan) powder diffractometer.

Synthesis of the monomers

The synthesis of the vinyl monomers is shown in Schemes 1 and 2. 4-(Hydroxyethoxy)benzoic acid (**1**), 4-(10-undecylen-1-yloxy)-4′-ethoxybenzoic acid (**2**), 4-(4-ethoxybenzoyloxy)-4′-hydroxybiphenyl (**3**), and 4-(10-undecylen-1-yloxy) benzoic acid (**4**) were prepared according to the procedures reported previously [34, 38, 39]. Structures of $\mathbf{M_1}$ and $\mathbf{M_2}$ were characterized with infrared and ^{1}H-NMR spectrum. The characteristics of the proton shift for $\mathbf{M_2}$ are shown in Fig. 1.

Scheme 1 Synthetic route of LC monomer

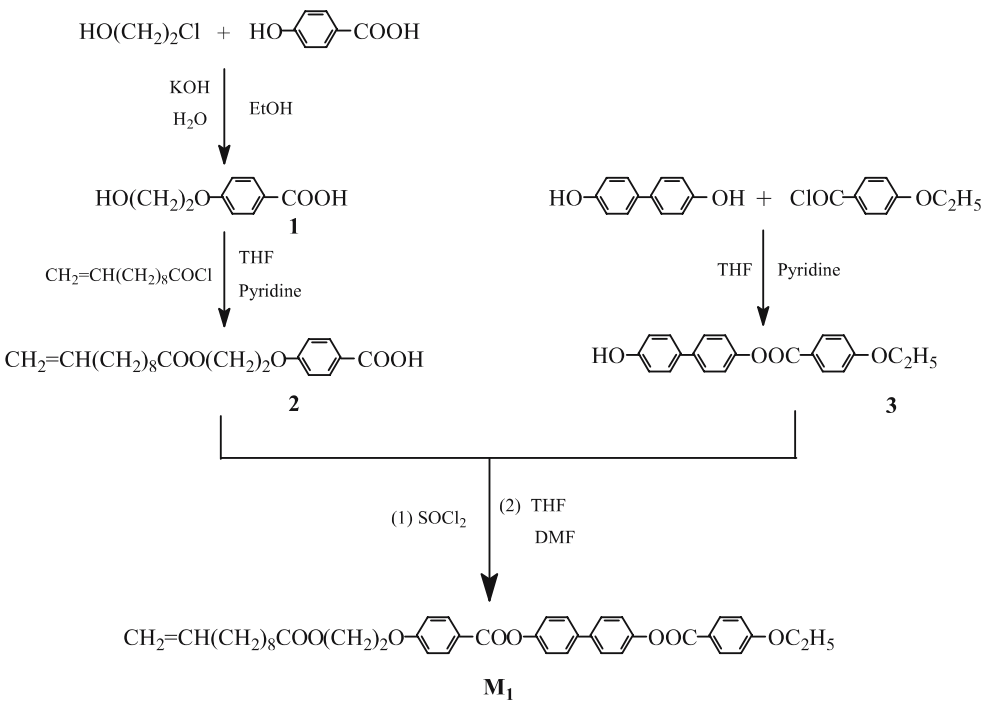

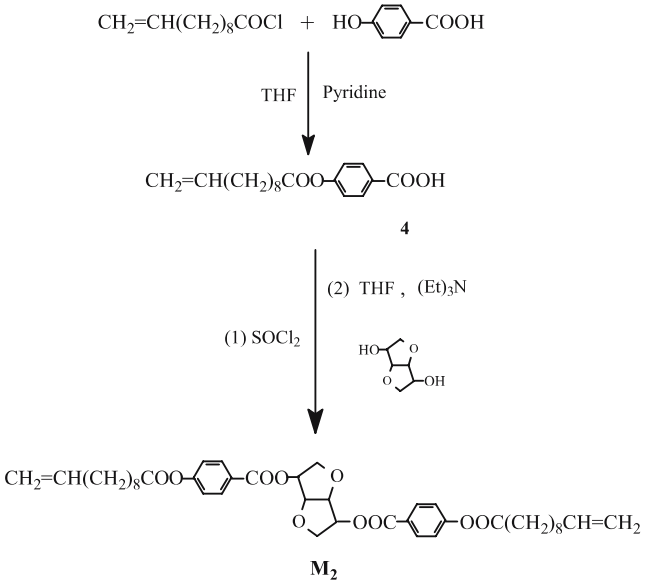

Scheme 2 Synthetic route of chiral crosslinking agent

*4-(4-Ethoxybenzoyloxy)biphenyl-4′-[(10-undecylen-1-yloxy)-4′-ethoxy]benzoate (**M**$_1$)*

4-(10-Undecylen-1-yloxy)-4′-ethoxybenzoyl chloride was prepared by reacting compound **2** with excess thionyl chloride according to the reported literature [39]. The acid chloride obtained (18.3 g, 0.05 mol), dissolved in 20 ml of tetrahydrofuran (THF), was added dropwise to a cold solution of compound **3** (17.2 g, 0.05 mol) in 100 ml of THF and 4 ml of *N*,*N*-dimethylformamide. The reaction mixture was heated to reflux for 16 h, cooled to room temperature, and then filtered. After concentrating the filtrate, the crude product was precipitated by the addition of water to the mixture and purified by recrystallization from isopropanol. Solid **M**$_1$ was obtained. Yield 62%, mp 117 °C. Infrared (KBr, cm^{-1}): 3,072 (=C−H); 2,925, 2,851 (−CH_3, −CH_2−); 1,747, 1,705 (C=O); 1,644 (C=C); 1,605, 1,512 (Ar−); 1,255 (C−O−C). ^{1}H-NMR ($CDCl_3$, TMS, δ, ppm): 1.25−1.75 [m, 15H, −C***H***$_3$ and −(C***H***$_2$)$_6$−]; 2.01 (m, 2H, CH_2=CHC***H***$_2$−); 2.53 (m, 2H, −CH_2C***H***$_2$COO−); 4.06 (t, 2H, −OC***H***$_2$$CH_3$); 4.33 (t, 2H, −$CH_2$C***H***$_2$O−); 4.65 (t, 2H, −COOC***H***$_2$−); 4.95−5.08 (dd, 2H, C***H***$_2$=CH−); 5.71−5.87 (m, 1H, CH_2=C***H***−); 7.02−8.18 (m, 16H, Ar−***H***). Elem. Anal. Calcd. for $C_{41}H_{44}O_8$: C, 74.07%; H, 6.67%. Found: C, 74.15%; H, 6.91%.

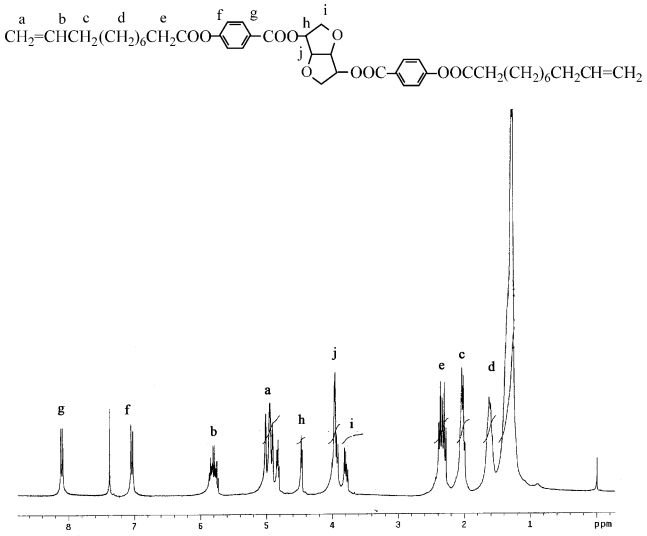

Fig. 1 ^{1}H-NMR spectrum of **M**$_2$

*Isosorbide di-(10-undecylen-1-yloxybenzoate) (**M**$_2$)*

4-(10-Undecylen-1-yloxy)benzoyl chloride (35.6 g, 0.11 mol) was dissolved in 20 ml of THF and then added dropwise to a cold solution of isosorbide (7.3 g, 0.05 mol) in 120 ml of THF and 14 ml of triethylamine. The mixture was refluxed for 16 h and cooled to room temperature, then filtered. After concentrating the filtrate, the residue was poured into cold water. The organic layer was washed with warm water, extracted by *n*-heptane and then dried with anhydrous magnesium sulfate. After removing *n*-heptane by distillation, the crude product was recrystallized from acetone. Solid **M**$_2$ was obtained. Yield: 76%, mp 85 °C, $[\alpha]_D^{20}$ −11.8° (toluene). Infrared (KBr, cm^{-1}): 3,074 (=C−H); 2,975, 2,855 (−CH_3, −CH_2−); 1,767, 1,738 (C=O); 1,641 (C=C); 1,602, 1,508 (Ar−); 1,250 (C−O−C). ^{1}H-NMR ($CDCl_3$, TMS, δ, ppm): 1.30−1.64 [m, 24H, −(C***H***$_2$)$_6$−]; 2.03 (m, 4H, CH_2=CHC***H***$_2$−); 2.41 (m, 4H, −CH_2C***H***$_2$COO−); 3.86 (t, 4H, −C***H***$_2$O−); 4.06 (m, 2H, −OC***H***<); 4.56 (m, 2H, −COOC***H***<); 4.89−5.03 (m, 4H, C***H***$_2$=CH−); 5.73−5.86 (m, 2H, CH_2=C***H***−); 7.02−8.05 (m, 8H, Ar−***H***). Elem. Anal. Calcd. for $C_{42}H_{54}O_{10}$: C, 70.17%; H, 7.57%. Found: C, 70.02%; H, 7.76%.

Synthesis of the elastomers

The synthesis of the elastomers **P**$_2$–**P**$_5$ is outlined in Scheme 3. Yields and polymerization are summarized in Table 1. For the synthesis of **P**$_2$–**P**$_5$, the same method was adopted. The synthesis of **P**$_3$ is described as an example. **M**$_1$, **M**$_2$, and **PMHS**, as shown in Table 1, were dissolved in 60 ml of freshly distilled toluene. The mixture was heated to 65 °C under nitrogen and anhydrous conditions, and then 2 ml of THF solution of H_2PtCl_6 catalyst (5 mg/ml) was injected with a syringe. The progress of the hydrosilylation reaction, monitored by the Si−H stretch intensity, went to completion as indicated by infrared. The elastomer **P**$_3$ was obtained and purified by several reprecipitations from toluene solution into methanol, and then dried in vacuum. The infrared spectra of **P**$_2$–**P**$_5$ showed the complete disappearance of the Si−H stretching band at 2,166 cm^{-1} and the olefinic C=C stretching band at 1,644 cm^{-1}.

Scheme 3 Synthesis and schematic representation of elastomers

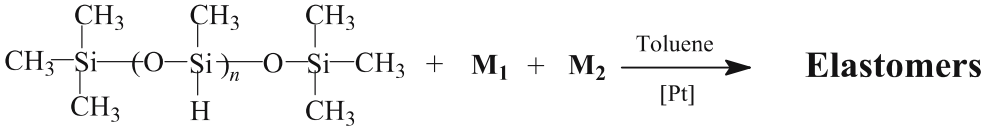

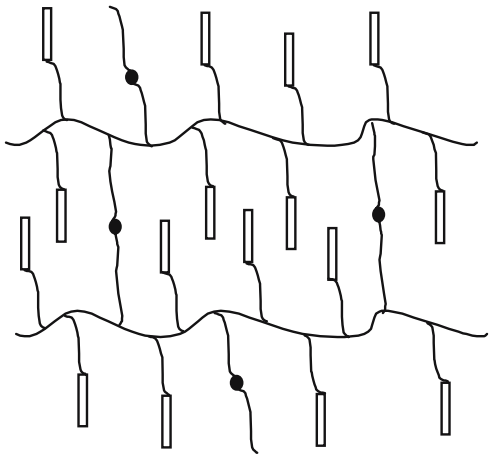

Results and discussion

Swelling properties

There are some ways to determine the effective crosslink density of elastomers, for example, methods of measuring the rubber elasticity or the swelling characteristics. We have studied these elastomers with the help of swelling experiments.

From swelling experiments, the crosslink density or the average molar mass of the network chains between two crosslinks, $\overline{M}_c$, was calculated according to the Flory swelling theory [40, 41],

$$\overline{M}_c = \rho_e \cdot V_1(0.5 - \chi_1)^{-1} \cdot q^{5/3} \quad (1)$$

where ρ_e is the density of the elastomer, V_1 is the molar volume of the swelling solvent, q is the equilibrium ratio of the volumes of the swollen and unswollen elastomers, and χ_1 is the Flory–Huggins parameter or the interaction parameter between the solvent and the elastomer.

The parameter χ_1 was calculated from the second Virial coefficient A_2 according to Eq. 2 [40],

$$\chi_1 = 0.5 - A_2 \cdot \rho_u^2 \cdot V_1 \quad (2)$$

where ρ_u is the density of the uncrosslinked polymer. From Eqs. 1 and 2, $\overline{M}_c$ was obtained.

The equilibrium ratio of the elastomer was determined with the following equation [40]:

$$q = 1 + (W_2/W_1 - 1) \cdot \rho_p \Big/ \rho_s \quad (3)$$

where W_1 and W_2 are the weights of the elastomers before swelling and at equilibrium swelling and ρ_p and ρ_s are the density of the polymer and solvent, respectively.

Swelling experiments were measured in 10 ml of toluene with 0.5 g of samples. The samples were placed into glass

Table 1 Yield, polymerization, and solubility

Polymer	Feed (mmol)			M_2^a (mol%)	Yield (%)	Solubility
	PHMS	M_1	M_2			toluene
P_1	1	7.00	0.00	0	84	+
P_2	1	6.46	0.27	4	81	−
P_3	1	5.96	0.52	8	82	−
P_4	1	5.72	0.64	10	79	−
P_5	1	5.50	0.75	12	82	−

+ Soluble, − insoluble or swelling
[a] Molar fraction of **M_2** based on (**M_1**+**M_2**)

Table 2 Physical properties of elastomers

Polymer	Density (g/cm^3)	q	$\overline{M}_c$ (g/mol)	Degree of swelling[a] (wt.%)
P_1	1.071	–	–	–
P_2	1.078	3.93	1,0550	350
P_3	1.086	3.22	7,625	310
P_4	1.088	2.89	6,380	280
P_5	1.093	2.52	5,101	260

[a] Toluene uptake in weight % at room temperature, referring to the weight of the extracted polymer.

Table 3 Phase transition temperatures of monomers

Monomer	Transition temperature in °C (corresponding enthalpy changes in $J \cdot g^{-1}$) $\frac{\text{heating}}{\text{cooling}}$
$\mathbf{M_1}$	$\frac{\text{K117.4(30.2)N174.8(2.6)I}}{\text{I173.3(1.7)N–K}}$
$\mathbf{M_2}$	$\frac{\text{K84.6(52.5)I}}{\text{164.5(66.3)K}}$

K Solid, *N* nematic, *I* isotropic

vial closed hermetically. They were subsequently homogenized at room temperature by strong shaking. Each vial was weighted before and after homogenization. After the vial was sealed, they were left in constant temperature insulated. Swelling experiment was accomplished in several days at room temperature to achieve equilibrium. Swollen elastomers removed from solvents at regular intervals were dried superficially with filter paper, weighed, and placed with the same condition. The measurements were continued until constant weight was reached for each sample. Table 2 shows swelling properties of the elastomers. As seen from the data listed in Table 2, with increasing concentration of crosslinking units in the networks, $\overline{M}_c$ and the degree of swelling reduced, that is to say, the crosslink density increased.

Mesomorphic properties

The mesomorphic properties of $\mathbf{M_1}$, $\mathbf{M_2}$ and $\mathbf{P_1}$–$\mathbf{P_5}$ were investigated with DSC, TGA, POM, and XRD. Their phase transition temperatures, corresponding enthalpy changes (ΔH), mesophase types, and thermal decomposition temperatures are summarized in Tables 3 and 4, respectively. Typical DSC curves of $\mathbf{M_1}$, $\mathbf{M_2}$, and $\mathbf{P_1}$–$\mathbf{P_5}$ are presented in Figs. 2, 3, and 4, respectively.

DSC heating thermograms of $\mathbf{M_1}$ showed a melting transition at 117.4 °C and a nematic to isotropic phase transition at 174.8 °C. However, the cooling thermogram of $\mathbf{M_1}$ only showed an isotropic to nematic phase transition at 173.3 °C, and a crystallization temperature did not appear due to the fast cooling temperature. DSC curves of $\mathbf{M_2}$ only showed a melting transition and a crystallization transition on heating and cooling cycles. Optical textures of the samples are studied by POM with hot stage. POM results showed that $\mathbf{M_1}$ exhibited an enantiotropic mesophase, and $\mathbf{M_2}$ revealed no texture and birefringence phenomenon on heating and cooling cycles. $\mathbf{M_1}$ displayed typical nematic threaded texture and droplet texture on heating and cooling cycles. The optical textures of $\mathbf{M_1}$ are shown in Fig. 5.

DSC heating thermograms of $\mathbf{P_1}$–$\mathbf{P_4}$ showed a glass transition at low temperature and a LC phase to isotropic transition at high temperature. In general, a low concentration of crosslinking did not significantly affect the phase behavior of the LCEs, and reversible mesophase transitions

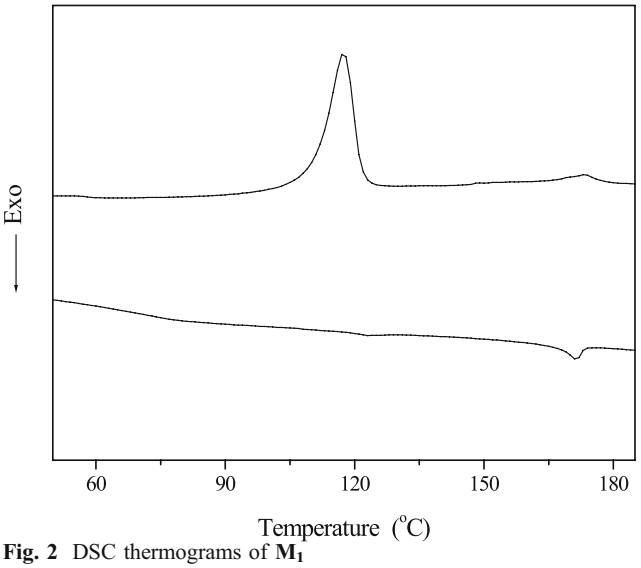

Fig. 2 DSC thermograms of $\mathbf{M_1}$

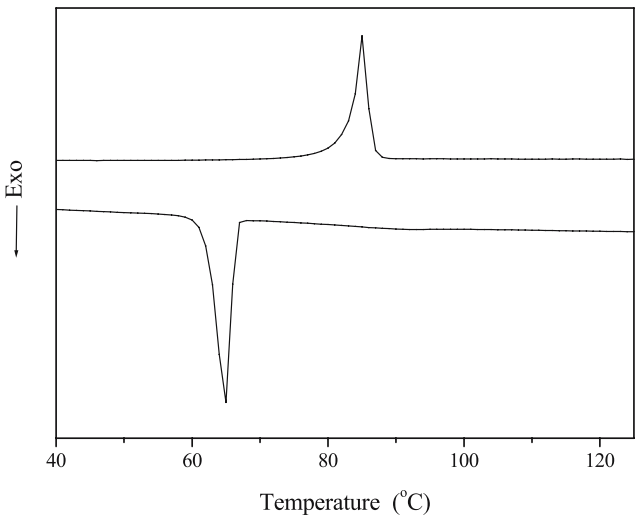

Fig. 3 DSC thermograms of $\mathbf{M_2}$

Table 4 Thermal properties of polymers

Polymer	T_g/ °C	T_i/°C	ΔH_i/ $J \cdot g^{-1}$	ΔT[a]	T_d[b]/ °C	Mesophase
$\mathbf{P_1}$	69.5	245.7	2.9	176.2	332.4	N
$\mathbf{P_2}$	66.4	234.3	2.6	167.9	339.2	Ch
$\mathbf{P_3}$	67.9	196.5	1.7	128.6	342.5	Ch
$\mathbf{P_4}$	72.6	174.4	0.9	101.8	344.7	Ch
$\mathbf{P_5}$	84.5	–	–	–	345.6	–

N Nematic, *Ch* cholesteric
[a] Mesophase temperature ranges (T_i–T_g)
[b] Temperature at which 5% weight loss occurred

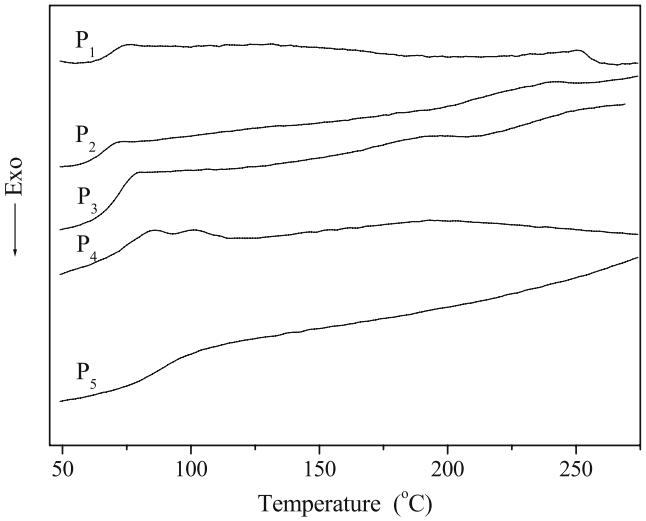

Fig. 4 DSC thermograms of $\mathbf{P_1}$–$\mathbf{P_5}$

were observed because there was enough molecular motion. In contrast, a high concentration of crosslinking had a strong influence on the LC behavior of the elastomers; it could cause the mesophase to disappear because of the depression of the LC orientational order. Therefore, DSC curves of $\mathbf{P_5}$ only showed a glass transition. This indicated that the LC properties began to disappear when the content of crosslinking units was greater than 10 mol%. POM results showed that $\mathbf{P_1}$ exhibited the threaded texture of nematic phase. The elastomer $\mathbf{P_2}$ exhibited oily streak texture of cholesteric phase, and $\mathbf{P_3}$ and $\mathbf{P_4}$ displayed stress-induced birefringence, which is similar to those described by Mitchell et al. [42], and they did not exhibit any LC textures because of elasticity. This indicated that the introduction of chiral crosslinking unit into the polymer could induce cholesteric phase. The optical texture of $\mathbf{P_1}$–

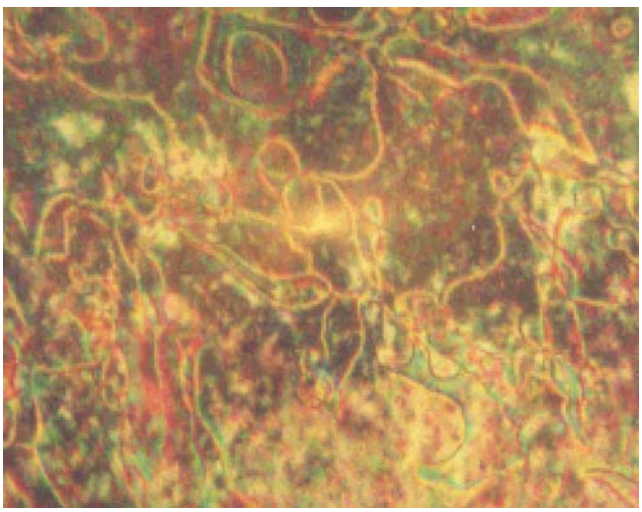

Fig. 5 Optical textures of $\mathbf{M_1}$ (200×): threaded texture on heating to 171.5 °C

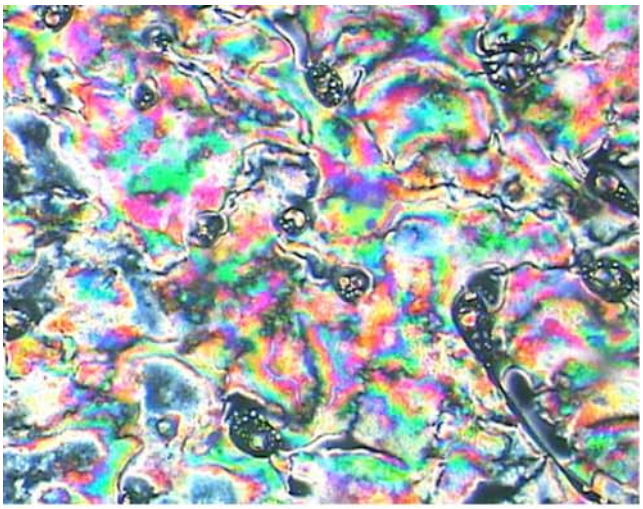

a

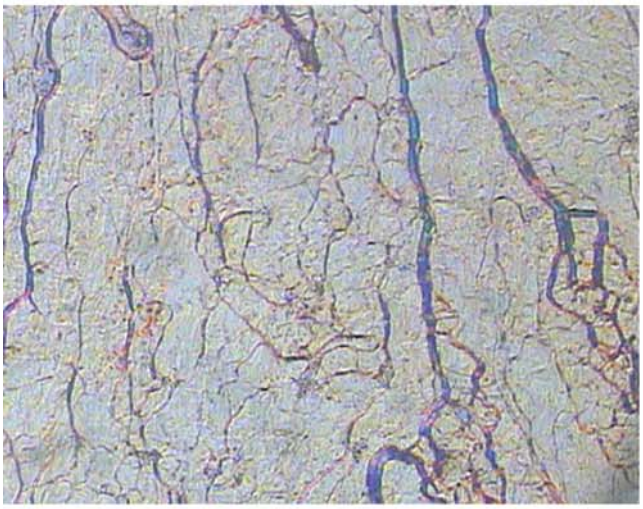

b

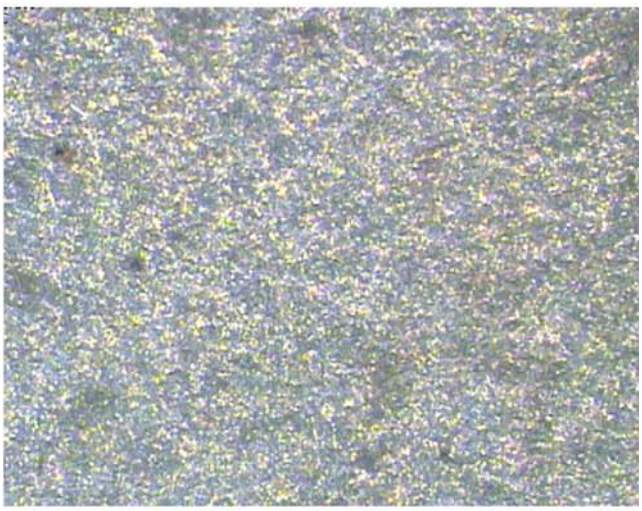

c

◀ **Fig. 6** Optical texture of $\mathbf{P_1}$–$\mathbf{P_3}$ (200×). **a** Nematic threaded texture of $\mathbf{P_1}$ at 235 °C; **b** cholesteric oily streak texture of $\mathbf{P_2}$ at 227 °C; **c** cholesteric texture of $\mathbf{P_3}$ at 125 °C

$\mathbf{P_3}$ is shown in Fig. 6. $\mathbf{P_5}$ showed only elasticity; this is consistent with the results obtained with DSC.

In general, chemical crosslinking imposes additional constraints on the motion of chain segments, makes free volume reduce, and causes an increase in the T_g. However, the effect may be small for weakly crosslinked polymers, and the T_g is also affected by the flexible crosslinking chains similar to the plasticization effect. The T_g of lightly crosslinked polymers may decrease. According to Table 4, compared with the T_g of $\mathbf{P_1}$, it was clearly seen that the T_g of $\mathbf{P_2}$ and $\mathbf{P_3}$ decreased by 3.1 to 1.6 °C. This indicated that the plasticization effect of the flexible crosslinking chains was predominant. However, general tendency was toward an increased T_g with increasing the crosslink density. The T_g of $\mathbf{P_2}$–$\mathbf{P_5}$ increased from 66.4 to 84.5 °C when the content of the crosslinking units increased from 4 to 12 mol%.

The chemical crosslinking also affected the T_i of LCEs. On one hand, the flexible crosslinking chains acted as diluent and led to a decrease in the T_i; on the other hand, chemical crosslinking could prevent the motion and orientation of mesogenic molecule at and in the vicinity of the crosslinking sites and did not favor the formation of mesogenic orientational order in the networks. Therefore, the T_i of LCEs decreased and disappeared with increasing crosslink density. The T_i decreased from 234.3 °C of $\mathbf{P_2}$ to 174.4 °C of $\mathbf{P_4}$ when the content of the crosslinking unit increased from 4 to 10%. In addition, $\mathbf{P_2}$–$\mathbf{P_4}$ displayed wide ΔT; however, ΔT decreased from 167.9 °C of $\mathbf{P_2}$ to 101.8 °C of $\mathbf{P_4}$ because the T_i decreased and the T_g increased.

The thermal stability of the elastomers was evaluated with TGA. The corresponding data are shown in Table 4. Figure 7 shows representative TGA curves of $\mathbf{P_2}$ and $\mathbf{P_4}$. TGA results showed that the temperatures at which 5% weight loss occurred (T_d) of the elastomers were greater than 330 °C; this indicated that the elastomers obtained had a high thermal stability. Moreover, as seen in Table 4, T_d of the elastomers increased with increasing content of crosslinking units.

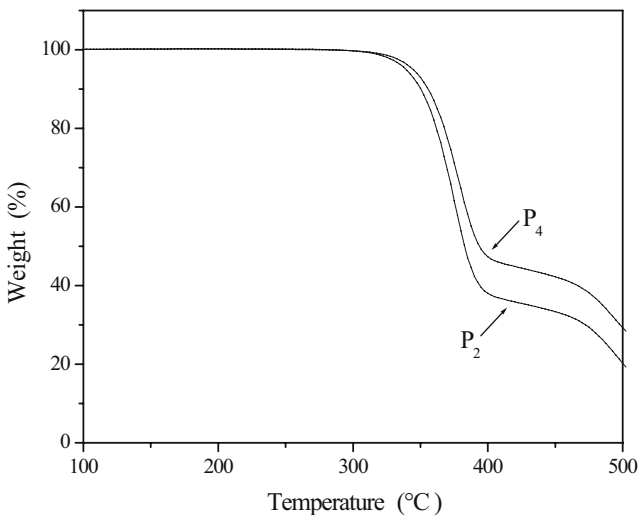

Fig. 7 TGA curves of $\mathbf{P_2}$ and $\mathbf{P_4}$

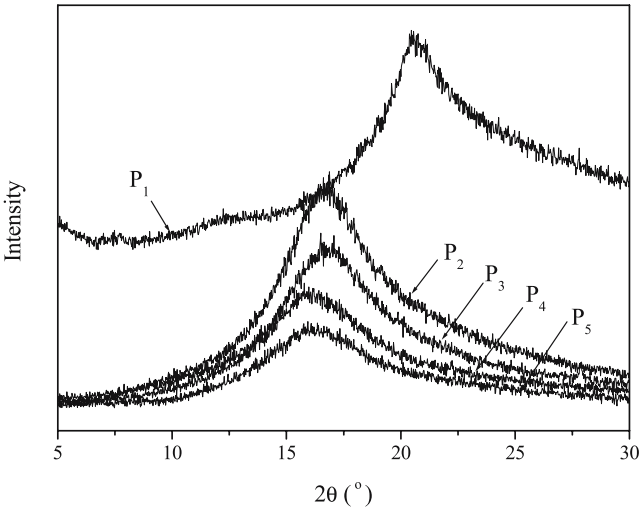

Fig. 8 XRD patterns of $\mathbf{P_1}$–$\mathbf{P_5}$

XRD studies were carried out to obtain more detailed information on the mesophase structure and type. In general, a broad peak associated with lateral packing at $2\theta \approx 20°$ in wide-angle X-ray diffraction (WAXD) curve occurs for nematic structure and a broad peak at $2\theta \approx 17°$ for cholesteric structure. Figure 8 shows representative XRD curves of $\mathbf{P_1}$ and $\mathbf{P_4}$ at 120 °C. A broad peak was observed at $2\theta = 20.6°$ for $\mathbf{P_1}$ and 16.8–17.4° for $\mathbf{P_2}$–$\mathbf{P_5}$ in WAXD curves, respectively. Moreover, a broad peak was more and more diffuse, and peak intensity decreased with increasing crosslink density, and this indicated the decrease of LC order from $\mathbf{P_2}$ to $\mathbf{P_4}$.

Conclusions

New nematic monomer $\mathbf{M_1}$, chiral crosslinking agent $\mathbf{M_2}$, and a series of side-chain cholesteric LCEs derived from an isosorbide derivate were synthesized and characterized. $\mathbf{M_1}$ and $\mathbf{P_1}$ exhibited nematic textures. $\mathbf{P_1}$–$\mathbf{P_4}$ showed very wide mesophase temperature ranges and high thermal stability. The elastomers containing greater than 10 mol% of crosslinking units only showed elasticity, and no LC phase was seen. For $\mathbf{P_2}$–$\mathbf{P_4}$, the T_g increased, T_i and ΔT decreased with increasing content of the crosslinking unit.

Acknowledgment The authors are grateful to National Natural Science Fundamental Committee of China, Natural Science Fundamental Committee of Liaoning Province, and Postdoctoral Science and Research Foundation of Northeastern University for financial support of this work.

References

1. Finkelmann H, Kock HJ, Rehage G (1981) Makromol Chem Rapid Commun 2:317
2. Hikmet RAM, Lub J, Higgins JA (1993) Polymer 34:1736
3. Sun SJ, Chang TC (1995) J Polym Sci A Polym Chem 33:2127
4. Symons AJ, Davis FJ, Mitchell GR (1999) Polymer 40:5365
5. Nair BR, Gregoriou VG, Hammond PT (2000) Polymer 41:2961
6. Li M, Hu ZJ, Chen G, Chen XF (2003) J Appl Polym Sci 88:2275
7. Shivakumar E, Das CK, Segal E, Narkis M (2005) Polymer 46:3363
8. Brehmer M, Zentel R (1995) Macromol Rapid Commun 16:659
9. Eckert T, Finkelmann H, Keck M, Lehmann W, Kremer F (1996) Macromol Rapid Commun 17:767
10. Ikeda Y, Yonezawa T, Urayama K, Kohjiya S (1997) Polymer 38:3229
11. Ortiz C, Ober CK, Kramer EJ (1998) Polymer 39:3713
12. Terentjev EM, Warner M (1999) Eur Phys J B 8:595
13. Gebhard E, Zentel R (2000) Macromol Chem Phys 201:902
14. Hirschmann H, Roberts PMS, Davis FJ, Guo W, Hasson CD, Mitchell GR (2001) Polymer 42:7063
15. Hiraoka K, Uematsu Y, Stein P (2002) Macromol Chem Phys 203:2205
16. Hiraoka K, Stein P, Finkelmann H (2004) Macromol Chem Phys 205:48
17. Bunning TJ, Kreuzer FH (1995) Trends Polym Sci 3:318
18. Peter PM (1998) Nature 391:745
19. Sapich B, Stumpe J, Kricheldorf HR (1998) Macromolecules 31:1016
20. Kim ST, Finkelmann H (2001) Macromol Rapid Commun 22:429
21. Finkelmann H (2001) Adv Mater 13:1069
22. Schmidtke J, Stille W, Finkelmann H (2003) Phys Rev Lett 90:083902
23. Cicuta P, Tajbakhsh AR, Terentjev EM (2002) Phys Rev E 65:051704
24. Bermel PA, Warner M (2002) Phys Rev E 65:056614
25. Kricheldorf HR, Probst N (1995) Macromol Rapid Commun 16:231
26. Kricheldorf HR, Sun SJ, Chen CP, Chang TC (1997) J Polym Sci A Polym Chem 35:1611
27. Sun SJ, Schwarz G, Kricheldorf HR, Chang TC (1999) J Polym Sci A Polym Chem 37:1125
28. Sun SJ, Liao YC, Chang TC (2000) J Polym Sci A Polym Chem 38:1852
29. Kricheldorf HR, Chatti S, Schwarz G, Krüger RP (2003) J Polym Sci A Polym Chem 41:3414
30. Lin Q, Pasatta J, Long TE (2003) J Polym Sci A Polym Chem 41:2512
31. Zhang BY, Zheng YY, Xu Y, Lu HW (2005) Liq Cryst 32:357
32. He XZ, Zhang BY, Hu JS, Tian M (2005) Liq Cryst 2(32):299
33. Hu JS, Zhang BY, Zheng YY, Li QY (2005) React Funct Polym 64:1
34. Hu JS, Zhang BY, AJ, Yang LY, Wang B (2006) Eur Polym J 42:2849
35. Hu JS, Zhang BY, Tian M, Ren SC, Guo DY (2005) Colloid Polym Sci 283:1349
36. Hu JS, Zhang BY, Guan Y (2004) J Polym Sci A Polym Chem 42:5262
37. Zhang BY, Hu JS, Wang Y, Qian JH (2003) Polym J 35:476
38. Hu JS, Zhang BY, YG, Wang Y (2003) Polym J 35:160
39. Hu JS, Zhang BY, Zhou AJ, Dong YL, Zhao ZX (2005) J Polym Sci A Polym Chem 43:3315
40. Folry PJ (1953) Principles of polymer chemistry. Cornell University Press, Ithaca, NY
41. Lffler R, Finkelmann H (1990) Makromol Chem Rapid Commun 11:321
42. Mitchell GR, Davis FJ, Ashman A (1987) Polymer 28:639